Research Article | Vol. 12, No. 6 / 1 June 2021 / Biomedical Optics Express 3338
Biomedical Optics EXPRESS

Optical design and performance of a trifocal sinusoidal diffractive intraocular lens

FIDEL VEGA,[1,*] MAITE VALENTINO,[1] FRANCO RIGATO,[2] AND MARÍA S. MILLÁN[1]

[1]*Departament d'Òptica i Optometria, Universitat Politècnica de Catalunya, BarcelonaTech, Violinista Vellsolà 37, 08222 Terrassa, Spain*
[2]*Horizons Optical S.L.U, Avenida Alcalde Barnils 72, 08174 Sant Cugat del Vallès, Spain*
[*]*fidel.vega@upc.edu*

Abstract: Two theoretical sinusoidal diffractive profile models to build up a trifocal intraocular lens (IOL) are analysed. Topographic features of the diffractive zones such as their shape, step height and radii, as well as the energy efficiency (EE) of the foci, depends on the particular model, and are compared to the ones experimentally measured in a trifocal lens that claims to be designed with a generic sinusoidal diffractive profile: the Acriva Trinova IOL (VSY Biotechnology, The Netherlands). The topography of the IOL is measured by confocal microscopy. The EE is experimentally obtained through-focus with the IOL placed in a model eye. The experimental results match very accurately with one of the theoretical models, the *optimum triplicator*, once that a spatial shift in the sinusoidal profile is introduced in the model.

1. Introduction

Pseudo-accommodation enabling good distance, intermediate and near vision without the need of additional refractive correction after cataract surgery is nowadays possible with presbyopia-correcting intraocular lenses (IOLs). In practice, advanced IOL designs extend the range of vision by means of either three distinct foci (trifocal IOLs), or an extended depth of focus (EDOF IOLs) [1]. EDOF lenses are intended to mitigate the photic phenomena (glare and halo) and the discontinuous visual transition for objects viewed at different distances, which are inherent to IOL designs with multiple of non-overlapping discrete foci. However, clinical results have shown that current EDOF IOLs do not extend enough the range of vision to provide the same sharpness of near vision as trifocal IOLs do [2,3]. In addition, it has been argued that objective dysphotopsia may not be significantly reduced compared to trifocal IOLs [4,5].

Trifocal IOLs are hybrid refractive-diffractive lenses formed by a base refractive lens plus a diffractive profile of concentric rings engraved on one of the lens surfaces. Foci for distance, intermediate and near vision are produced by the combination of the high optical power of the base refractive lens plus the low additional powers associated with the diffraction orders generated by the diffractive profile. Thus, the design of the diffractive element (e.g., shape, step height and radii of the diffractive zones) is of paramount importance since it determines the optical power of the different foci (in other words, the addition in diopters of the IOL), the chromatic behavior of the IOL, the intensity assigned to each focus and the energy efficiency (EE) through the range of vision [6–10]. Paradoxically, few papers [11–15] have reported experimental measurements of the topographic features of diffractive IOLs and have analyzed to what extent these measurements agree with the theoretical profiles the lenses are supposed to be based on.

In their comprehensive paper Loicq *et al*. [12] have experimentally shown that several trifocal diffractive IOL designs available so far on the market (e.g. FineVision POD F, FineVision HP POD F GF, FineVision PODLGF -PhysIOL, S.A- and AT Lisa tri 839MP -Carl Zeiss, Meditec AG) are a combination of two bifocal diffractive patterns. Theoretical studies proposing bifocal diffractive profiles of different shape (kinoform, parabolic, binary. . .) can be found in [6,16,17].

#421942 https://doi.org/10.1364/BOE.421942
Journal © 2021 Received 4 Feb 2021; revised 26 Apr 2021; accepted 26 Apr 2021; published 12 May 2021

Biomedical Optics EXPRESS

An alternative to obtain a trifocal IOL with a single diffractive pattern relays on a sinusoidal profile incorporating amplitude modulation techniques as theoretically described in [18] and [19]. The approach presented in [18] was generalized by SokowŁowski *et al*. [8] by the appropriate selection of the modulation depth of a sinusoidal pattern to propose an IOL with up to seven foci. Osipov *et al*. [15] proposed a nonlinear transformation of the sinusoidal phase function reported in [18] to modify the intensity distribution among the diffraction orders of a zone plate.

To our knowledge, there is only a commercially available example of IOL that claims to be designed according to a sinusoidal diffractive profile: the Acriva Trinova IOL (VSY Biotechnology, The Netherlands) [20]. We have found only one paper [21] reporting a comparison of clinical outcomes between Acriva Trinova and FineVision but there are no publications that describe in detail the diffractive profile of this lens and relate it to its optical behavior. Therefore, the aim of this study is the experimental characterization of the diffractive profile of the Acriva Trinova IOL and to compare its features (shape, step height, radii. . .) to the ones derived from theoretical sinusoidal diffractive profiles reported in earlier works [18,19]. In addition, to get further insight of the advantages and limitations that a sinusoidal profile design may have, we have studied in-vitro on a model eye, the optical performance of the Acriva Trinova IOL.

2. Materials and methods

2.1. Trifocal IOL with sinusoidal diffractive pattern

We assume a model of a refractive-diffractive trifocal IOL formed by a thin refractive lens (base lens) of optical power P_r and a sinusoidal diffractive profile engraved into one of the lens' surfaces. The phase function of such a sinusoidal profile takes the form $tan^{-1}(b\cos(2\pi a\, r^2))$ or $b\cos(2\pi a\, r^2)$, where r is the radial coordinate along the lens aperture, a and b are constants, and the cosine can be equivalently replaced by a sine function. A continuous and smooth profile characterizes this diffractive lens, which shows some advantages over sawtooth or stepped designs, such as shallower profiles with wider spaces between neighbor diffractive rings that should be lesser subject to debris accumulation [22]. The IOL is immersed in a medium with refractive index that corresponds to both, the aqueous and vitreous humors. Under monochromatic light illumination, the refractive indices of the lens and medium are n_L and n_A respectively.

The sinusoidal diffractive profile is intended to generate three diffraction orders m= -1, 0 and +1 with associated powers:

$$P_d(m) = m\, P_d\,, \tag{1}$$

P_d being usually referred to as the addition or add power of the IOL. We recall that *negative* orders are divergent and *positive* orders are convergent. Thus, the refractive-diffractive IOL is able to produce three foci for distance (m=-1), intermediate (m=0) and near (m=+1) vision with optical powers of P_r-P_d, P_r and P_r+P_d, respectively.

The diffractive profile $h(r)$, designed at wavelength λ, and the induced phase shift function $\Phi(r)$ are related by:

$$\Phi(r) = \frac{2\pi}{\lambda}\,(n_L - n_A)\,h(r)\,, \tag{2}$$

where r is the radial coordinate outwardly from the center of the lens and whose maximum value is the radius R of the lens. In the following, we assume λ=550 nm and refractive indices n_L=1.462 and n_A=1.336.

Two different sinusoidal phase shift functions will be analysed, and the parameters derived from this analysis will be compared to an example of commercially available sinusoidal IOL: the Acriva Trinova lens.

Biomedical Optics EXPRESS

2.2. Model 1: equienergetic trifocal

An equienergetic trifocal IOL proposed by Valle *et al.* [18], and referred from now on as Model 1, is represented by a phase function with the expression:

$$\Phi(r) = \beta \cos(2\pi \frac{r^2}{T}) , \tag{3}$$

where T (mm^2) is the period or pitch of the diffractive profile in r^2 space and determines the add power P_d of the trifocal IOL, which can be approached by:

$$P_d = \frac{2\lambda}{T} , \tag{4}$$

when $P_d << P_r$. The circularly symmetric diffractive profile is formed by annular concentric zones of radii:

$$r_n^2 = \frac{T}{2} + (n-1)\, T , \tag{5}$$

where n is an integer ≥ 1 that corresponds to the n^{th} zone. For example, in the case of a lens of P_d=1.5 D, Eqs. (4) and (5) yield to T=0.733 mm^2 and r_1=0.61 mm (radius of the first diffractive zone) respectively.

With regard to the β (rad) parameter in Eq. (3), it modulates the phase shift and eventually controls the diffraction efficiency of the m=0, and ±1 orders [8] and as a consequence, the energy distribution among the three foci. The parameter β is related to the maximum step height of the diffractive profile $h_{\max}$ by:

$$\beta = \frac{2\pi}{\lambda} (n_L - n_A)\, h_{\max} . \tag{6}$$

From the phase shift function given by Eq. (3), the diffraction efficiency of the m=0, and ±1 orders is [8,18]:

$$\eta_m = [J_m(\beta)]^2, \tag{7}$$

where J_0 and $J_{\pm 1}$ are the zero and first order Bessel functions respectively. β values in the vicinity of zero (or equivalently, with small values for the maximum step height $h_{\max}$) yields to ${J_0}^2$ values of ≈1.0 (100%), which corresponds to a monofocal IOL that would prioritize the 0$^{\text{th}}$-order focus at the cost of the positive and negative 1$^{\text{st}}$-order. The opposite occurs if $\beta \approx 2$ rad, a condition for which the IOL would be in practice a bifocal lens with distance (m=-1) and near (m=+1) foci of equal efficiencies (${J_{\pm 1}}^2 \approx 0.36$, 36%) and a 0$^{\text{th}}$-order (intermediate focus) of very low energy (${J_0}^2 \approx 0.05$, 5%). The condition for equal energy distribution among the three orders, i.e., $[J_0(\beta)]^2 = [J_{\pm 1}(\beta)]^2$, yields to diffraction efficiencies of 0.30 (30%) for each focus and happens when β=1.4376 rad [8,18]. This value leads to $h_{\max}$=1.0 μm (Eq. (6)) for the design wavelength λ=550 nm and refractive indices n_L=1.462 and n_A=1.336. The resultant sinusoidal diffractive profile $h(r)$,

$$h(r) = \frac{\lambda}{(n_L - n_A)} \frac{\beta \cos(2\pi \frac{r^2}{T})}{2\pi} = h_{\max} \cos(2\pi \frac{r^2}{T}) , \tag{8}$$

corresponding to equienergetic m=0, and ±1 diffraction orders, is illustrated in Fig. 1 in the case of an IOL of radius R=3 mm. The profile has a peak-to-valley height of $2h_{\max}$=2.0 μm and at the centre of the lens aperture (r=0), the step height h_0 coincides with $h_{\max}$.

Biomedical Optics EXPRESS

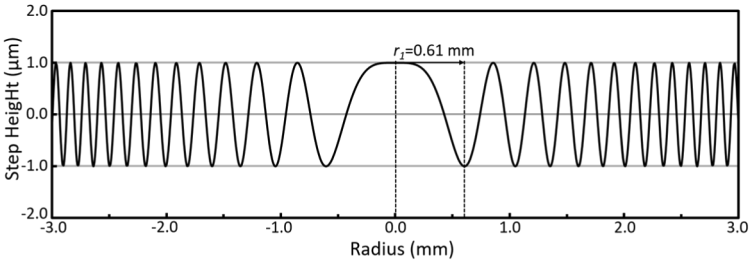

Fig. 1. Model 1 diffractive profile generated according to Eq. (8) (λ=550 nm, n_L=1.462, n_A=1.336, P_d=1.5 D, T=0.733 mm^2, and β=1.4376 rad). The radius r_1 of the first diffractive zone is shown.

2.3. Model 2: optimum triplicator

The second sinusoidal diffractive model (Model 2) analysed in this work is the *optimum triplicator* proposed by Gori *et al.* [19] whose phase function is:

$$\Phi(r) = \tan^{-1}\left(\alpha \sin(2\pi \frac{r^2}{T})\right) . \tag{9}$$

Using the relationship given in Eq. (2) it is straightforward to obtain the expression of the diffractive profile:

$$h(r) = \frac{\lambda}{(n_L - n_A)} \frac{\tan^{-1}\left(\alpha \sin(2\pi \frac{r^2}{T})\right)}{2\pi} , \tag{10}$$

where similarly to the Model 1, the parameter T is the period or pitch of the diffractive profile in r^2 space which in turn is related to the add power of the IOL P_d by Eq. (4). We highlight that with this model, the step height at the centre of the lens aperture (r=0) is h_0=0 µm while the radii of the diffractive zones are given by:

$$r_n^2 = \frac{3T}{4} + (n-1)\,T . \tag{11}$$

Thus, the radius of the first zone would be $r_1 = 0.74$ mm for a diffractive lens with the same add power P_d=1.5 D (T=0.733 mm^2) as considered in Model 1.

The parameter α governs the amount of energy distributed to the foci of the IOL because the diffraction efficiency of the m=0, and ±1 orders depend on α through the expressions [19]:

$$\eta_0 = \left[\frac{2}{\pi} K(-\alpha^2)\right]^2 , \tag{12}$$

and

$$\eta_{\pm 1} = \left[\frac{2}{\pi\alpha}\left(E(-\alpha^2) - K(-\alpha^2)\right)\right]^2 , \tag{13}$$

where K and E designate the complete elliptic integrals of first and second kind [23], respectively. Gori *et al.* [19] showed that the three orders can achieve equal diffraction efficiency of 0.308 (i.e., $\eta_0 = \eta_{\pm 1}$=0.308 (30.8%)) when α=2.65718, which requires that the maximum step height of the diffractive profile $h_{\max}$ be:

$$h_{\max} = \frac{\lambda}{(n_L - n_A)} \frac{\tan^{-1}(\alpha)}{2\pi} = 0.84\,\mu m , \tag{14}$$

The diffractive profile corresponding to the Model 2 (Eq. (10)) for an IOL of radius R=3mm is shown in Fig. 2, and evidences three distinct features in comparison to Model 1 (Fig. 1):

Biomedical Optics EXPRESS

- The radius of the first diffractive zone is slightly larger (0.74 mm versus 0.61 mm).
- The maximum step height h_{max} is significantly lower (0.84 μm versus 1.00 μm), which leads to a 16% shallower diffractive profile.
- The shape of the first diffractive zone shows a dip at the centre of the lens (r=0 mm).

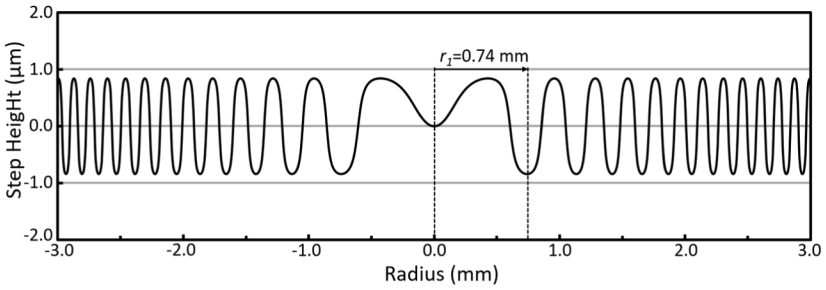

Fig. 2. Model 2 diffractive profile generated according to Eq. (10) (λ=550 nm, n_L=1.462, n_A=1.336, P_d=1.5 D, T=0.733 mm^2, and α=2.65718). The radius r_1 of the first diffractive zone is shown.

A more general form of Model 2 has been recently proposed in [24]. This generalized Model 2 introduces in the sine function a shift in radial direction, and therefore the diffractive profile is:

$$h(r) = \frac{\lambda}{(n_L - n_A)} \frac{\tan^{-1}\left(\alpha \sin\left(2\pi \frac{r^2 - S}{T}\right)\right)}{2\pi}. \tag{15}$$

The shift parameter S (mm^2) permits on the one hand, a fine tune of the radius r_1. For instance, Fig. 3 shows two profiles generated with S values of -0.060 and +0.307 mm^2 to match a radius r_1 of 0.70 mm (a case of interest concerning the design of the Acriva Trinova IOL as we will discuss later).

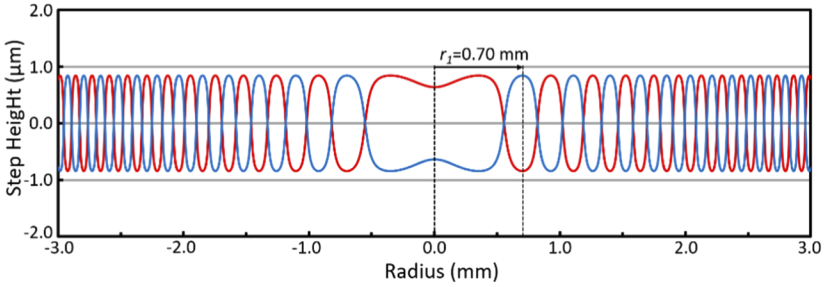

Fig. 3. Diffractive profiles generated according to Eq. (15) by introducing a shift S of -0.060 mm^2 (red line) and +0.307 mm^2 (blue line) to have a radius r_1 of 0.70 mm (λ=550 nm, n_L=1.462, n_A=1.336, P_d=1.5 D, T=0.733 mm^2, and α=2.65718).

Moreover, as it is evidenced in Fig. 3, the parameter S also has a considerably effect upon the shape of the first zone of the diffractive profile of the IOL. More in concrete, it changes the sign of the slope of the diffractive step, which turns out to provide an additional degree of freedom to (moderately) change the relative amount of energy split between the ±1 diffraction orders (i.e., between the distance and near foci) [24]. Noteworthy, since the parameter α is independent of S, the value of the maximum step height h_{max} (Eq. (14)) keeps constant in the generalized Model 2.

Biomedical Optics EXPRESS

2.4. Intraocular lens

To confront the proposed models with a commercially available IOL, we have considered the Acriva Trinova lens (VSY Biotecnology, The Netherlands) that claims to be designed with a sinusoidal profile whose features have not been disclosed by the manufacturer. The theoretical sinusoidal profiles shown above and the parameters (radii of the diffractive zones, maximum step height, etc. . .) derived from the different models, are compared with those measured experimentally in the Acriva Trinova IOL, besides the different powers of each focus.

The Acriva Trinova trifocal IOL has a hybrid diffractive-refractive design. The sinusoidal diffractive part, located on its anterior surface, consists of a central disk -also referred to as first diffractive zone- plus 11 concentric rings. It provides an addition of +1.5 D for the intermediate focus and +3.0 D for the near focus (in the IOL plane). The posterior surface is purely refractive. According to the manufacturer, the asphericity of the lens provides a 'mild correction' of the spherical aberration (SA), but to our knowledge, they have not reported yet any quantitative information about the SA Zernike coefficient. The lenses used in this study had 20 D of power for distance vision. Other specifications are listed in Table 1.

Table 1. Data of the Acriva Trinova IOL[a]

Material	Hydrophilic and hydrophobic acrylic copolymer
Refractive Index Wet	1.462 ± 0.002 (at 35°C)
Abbe Number	58
Optic Design	Trifocal sinusoidal
Optic Size	6.0 mm
Central disk radius	0.7 mm
Light Distribution (Photopic Conditions)	41% Far, 30% Intermediate, 29% Near

[a]Specifications provided by the manufacturer [20].

2.5. Surface topography

The surface topography of the Acriva Trinova IOL was measured by confocal microscopy (PLμ, Sensofar, Spain). The microscope generates a three-dimensional (3D) image of a region of the lens surface with the diffractive profile from a stack of 360 images acquired through a high-resolution Z-scan of 180 μm in the vertical direction. The field of view of a single image was 0.69×0.51 mm^2. The lens was held in a high-precision XY motorized platform which allows to acquire images across the whole surface of the lens. Automatic image stitching is performed by the software of the microscope to display a compound image representative of a large area of the IOL. From the 3D surface images, the best fitted sphere was subtracted to isolate the sinusoidal diffractive profile of the lens and obtain the height of the diffractive steps with ±0.10 μm accuracy. Moreover, the radii of the diffractive zones were experimentally measured from the distances between consecutive steps in the profile. These radii were additionally measured with a high resolution conventional optical microscopy (Axio Imager.M2, Zeiss). Both sets of radii measurements were in good agreement with maximum experimental differences smaller than 4% occurring for the outer rings.

2.6. Experimental setup and metrics

To analyze the optical performance of the Acriva Trinova IOL, the lens was placed in an optical bench with a model eye that followed the recommendations of the International Organization for Standardization (ISO) 11979–2:2014 [25]. The artificial cornea of our model eye induced +0.27 μm of 4th-order spherical aberration (5.2 mm pupil at the IOL plane) to mimic an average human cornea [26,27].

Biomedical Optics EXPRESS

The optical bench setting has been described in detail in former works [7]. In brief, it is formed by the illumination system, the model eye consisting of the cornea lens described above plus an iris diaphragm and a wet cell with the IOL, and the image acquisition system. A narrow-band green LED (λ=530 ± 20 nm) illuminated a 200 µm pinhole test, which was placed in the object focal plane of a 200 mm collimator lens. This way, the pinhole test is optically set to infinity for the model eye. A diaphragm used as entrance pupil, limited the IOL aperture to 3.0 and 4.5 mm. The model eye with the IOL formed aerial images of the pinhole test at their distance, intermediate and near foci. These images were sequentially magnified and captured by an infinity corrected 10X microscope assembled to an 8-bit CCD camera. This image acquisition system was mounted on high resolution XYZ translation holders. Through-focus image acquisition was performed by scanning the image space with the microscope in steps of 0.1 D, covering a range of approximately 7.0 D.

The image recorded at each focal plane consisted of the focused image of the pinhole (core), surrounded by a blurred halo due to the overlapping of the unfocused images coming from the other foci. The optical performance of the Acriva Trinova IOL was evaluated through-focus (TF) by calculating the energy efficiency (EE) of each image by the light in the bucket (LIB) metric [28] that quantifies the total amount of light located in the central core of the point spread function (PSF) relative to that in a monofocal diffraction-limited PSF [29]. Armengol *et al*. [30], have recently shown the potential of the LIB metric as a preclinical predictor of the postoperative visual acuity. The method to experimentally measure the LIB, firstly applies an edge detection algorithm to segment the pinhole core image. Then, it determines the percentage of energy that falls in the core (I_{core}) with respect to the total energy contained in the image ($I_{total} = I_{core} + I_{halo}$). The EE is calculated by the ratio I_{core} / I_{total}, which is easy to compute in the experimental practice. The application of the LIB metric to a nonpoint object, like the 200 µm pinhole used in this study, was justified elsewhere [9].

3. Results

3.1. Intraocular lens surface topography

Figure 4 shows an optical image of the Acriva Trinova IOL anterior surface with the diffractive rings (Fig. 4(a)) and two topographical sections (Fig. 4(b)) obtained with the confocal microscopy after removing the main curvature of the lens.

The topographical measurements evidence sinusoidal-like steps in the diffractive profile but for the central disc, which appears as a depressed, relative flat region.

Experimental cross section profiles obtained from the 3D confocal topographies are shown in Fig. 5 jointly with the sinusoidal diffractive profile generated with the generalized Model 2 with a positive S value (S=+0.307 mm^2 in Eq. (15) and Fig. 3 blue line). These results confirm a remarkable similarity between the shape of the experimental and simulated profiles, both displaying a pattern of a central disk and 11 sinusoidal steps in the 3 mm radius of the IOL optic zone.

An experimental maximum step height of h_{max}=0.78 ± 0.10 µm was obtained from the average of the height values of the 12 steps measured by confocal microscopy. Taking into account the experimental uncertainty, this value matches the 0.84 µm step height derived from Eq. (14) with the theoretical Model 2.

3.2. Radii of the diffractive zones

Given the similarity found between the experimental diffractive profile of the Acriva Trinova IOL with the one corresponding to the generalized Model 2 with positive S shift (Fig. 5), we have compared the experimental values of the radii of the 12 diffractive zones with the ones deduced with said Model 2 with positive S shift (Fig. 6).

Biomedical Optics EXPRESS

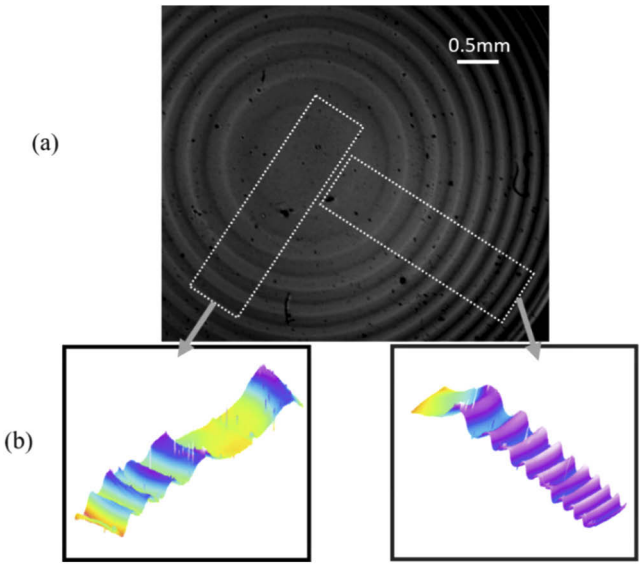

Fig. 4. (a) Optical image of the surface of the Acriva Trinova IOL showing the diffractive rings and (b) 3D confocal microscopy topographies of the rectangular sections indicated in (a).

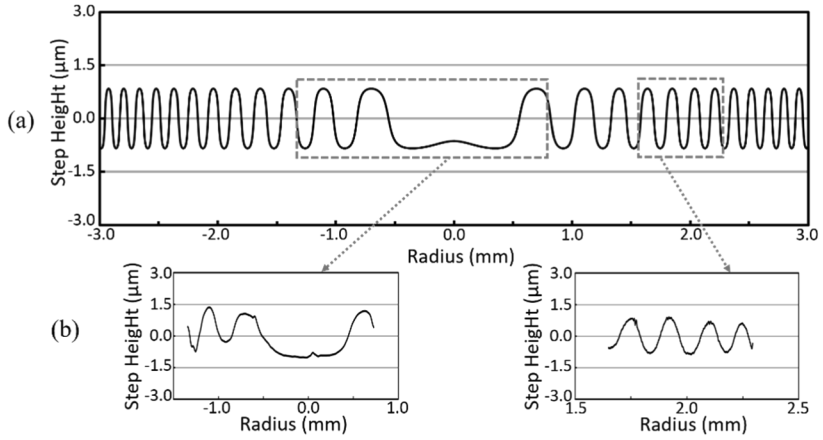

Fig. 5. (a) Theoretical sinusoidal diffractive profile generated according to Model 2 with shift S of 0.307 mm^2 in Eq. (15) (λ=550 nm, n_L=1.462, n_A=1.336, P_d=1.5 D, T=0.733 mm^2, and α=2.65718). (b) Experimental profile sections of the center (left) and outer rings (right) of the Acriva Trinova IOL.

Biomedical Optics EXPRESS

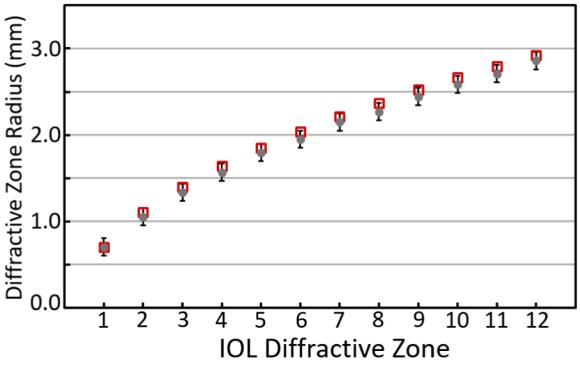

Fig. 6. Predicted (red □) and experimental (grey •) radii of diffractive zones of the Acriva Trinova IOL. Theoretical radii are derived from the generalized Model 2 with S =+0.307 mm^2. Error bars are ±0.02 mm.

The experimental radius of the first zone was r_1=0.70 ± 0.02 mm, which is in excellent agreement with both, the value provided by the manufacturer (Table 1) and the one derived from Model 2 with S = +0.307 mm^2. Moreover, the radii predicted by this model for the rest of diffractive rings closely replicates the values of the experimental ones as probed in Fig. 6.

3.3. *Optical characterization of the lens: through-focus energy efficiency*

Figure 7 shows the pinhole images at the near, intermediate and distance foci of the model eye with the Acriva Trinova IOL. The three images appear quite similar which qualitatively evidences a balanced energy distribution among the foci.

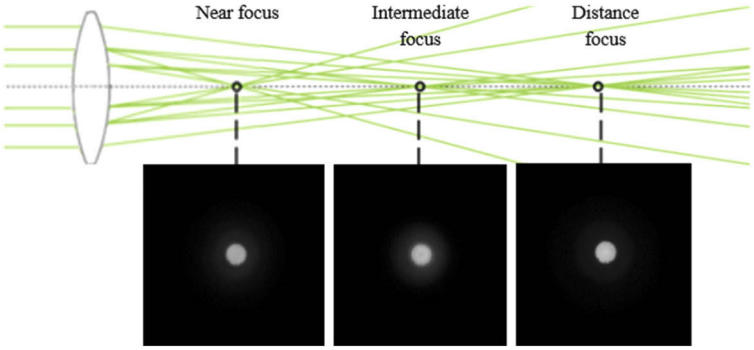

Fig. 7. Top: Schematic drawing representating a trifocal IOL. Bottom: Experimental images of the pinhole object formed at the three foci by the model eye with the trifocal Acriva Trinova IOL (λ = 530 nm, 3.0 mm pupil).

The experimental through-focus energy efficiency (TF-EE) curves obtained with two pupil diameters (3.0 and 4.5 mm) are represented in Fig. 8 and further confirm this trend. With the smallest pupil (3.0 mm), the TF-EE distribution results in a smooth curve across the analysed dioptric range, with the peak for distance vision showing slightly higher EE values than the intermediate and near ones. These peaks are experimentally located at dioptric powers of 20.2 ± 0.1 D (distance), 21.5 ± 0.1 D (intermediate) and 22.9 ± 0.1 D (near).

As the pupil increases to 4.5 mm, the three EE peaks become somewhat more evident, they are slightly shifted towards higher power, and overall, there is a decrease of the TF-EE for all dioptric powers.

Biomedical Optics EXPRESS

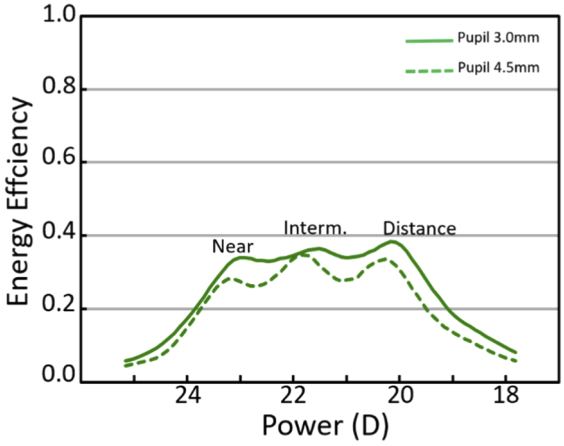

Fig. 8. Experimental through-focus energy efficiency (TF-EE) curves of the Acriva Trinova IOL obtained with pupil diameters of 3.0 mm (continuous line) and 4.5 mm (dashed line).

4. Discussion

Trifocal diffractive IOL designs have been commonly based on a refractive (or base lens) of refractive power P_r, plus the combination of two bifocal diffractive profiles which split light into 0^{th} and $+1^{st}$ diffraction orders of different add power. The bifocal profiles with a kinoform shape [17] (also referred to as parabolic after making a paraxial approximation) [6], are designed with periods (in r^2 space) of T and $T/2$. Then, according to Eqs. (1) and (4), the $+1^{st}$ diffraction orders produced by these profiles have addition powers of P_d and $2P_d$ respectively, while their 0^{th} orders do not have associated any power. The joint effect of the base lens and the two bifocal profiles is the formation of three foci: distance, intermediate and near with powers P_r, P_r+P_d and P_r+$2P_d$ respectively. An example of such design with reported add powers of +1.75 D (intermediate) and +3.50 D (near) is provided in [11] and has been implemented in several models of the FineVision (PhysIOL) family of IOLs.

Alternatively, there is also the possibility to efficiently generate three foci with just a single diffractive profile. For instance, Lenkova [31] describes a theoretical refractive-diffractive IOL with a binary profile that is similar to a phase zone plate, which diffracts light into m = -1, 0 and +1 orders with powers P_r-P_d, P_r and P_r+P_d, to form the distance, intermediate and near foci of the lens respectively. The radii of the diffractive zones in the binary profile are defined by: ${r_n}^2=n$ T, being $T=\lambda/P_d$, the required period (r^2 space) to have the addition power P_d. The diffraction efficiency of the m=0, and ±1 orders depends on the β parameter defined in Eq. (6) and thus, on the step height of the binary profile, through the expressions [32]:

$$\eta_0 = \left[\cos\left(\frac{\beta}{2}\right)\right]^2, \tag{16}$$

and:

$$\eta_{\pm 1} = \left[\left(\frac{2}{\pi}\right)\sin\left(\frac{\beta}{2}\right)\right]^2. \tag{17}$$

Using Eqs. (16) and (17) it is straightforward to obtain that such binary profile can produce three orders (or foci) with the same diffraction efficiency of 28.8% when β=2.0078 rad, and thus, ideally 86.4% of the incoming light energy would be used in the vision process. The remaining (13.6%) would go into higher positive and negative orders not useful for vision purposes. A binary diffractive profile has been implemented in the flat surface of a plano-convex trifocal

Biomedical Optics EXPRESS

IOL: the MIOL-Record (Reper-NN Company) [33]. Noteworthy, instead of diamond turning which is the common method to fabricate multifocal IOLs, high-precision fabrication of the steep slopes (ideally infinite slopes) of the binary profile, requires a more complex multistep process [32]. A sinusoidal diffractive profile with more gentle slopes overcomes this handicap while still producing three foci with relative high efficiency.

We have analysed two well-stablished theoretical sinusoidal diffractive profiles reported in earlier works: Model 1 corresponding to Eq. (8), was proposed by Valle *et al.* in [18], while Model 2 described by Eq. (10), was originally presented by Gori *et al.* [19] and more recently reformulated in [24] by adding a shift parameter to the radial coordinate (Eq. (15)). The features (profile shape, step heights, zone radii. . .) derived from these theoretical models have been compared to the experimental values obtained by confocal and optical microscopy from a commercially available IOL that claims to be "the world's first and only sinusoidal trifocal IOL", the Acriva Trinova lens. In addition, we have studied *in-vitro* on a model eye, the optical performance of the Acriva Trinova IOL to get further insight of the advantages and limitations that a sinusoidal profile design may have, with especial emphasis on the energy split to the foci and through-focus.

With both models and similarly to the case of the binary profile, the incoming light is diffracted into m = -1, 0 and +1 orders with powers P_r-P_d, P_r and P_r+P_d, to form the distance, intermediate and near foci of the lens. According to the manufacturer, the Acriva Trinova has add powers (relative to the distance focus) of +1.5 and +3.0 D to provide clear vision at intermediate and near distances. Since the lens studied in this work had an optical power for distance of 20.0 D (corresponding to a base power P_r=21.5 D minus the add power P_d=1.5 D), one would expect to have peaks of optical quality and energy efficiency at 20.0 D (distance), 21.5 D (intermediate) and 23 D (near). The experimental through-focus energy efficiency results (Fig. 8) confirm the occurrence of three peaks of optical quality at powers in close agreement with the expected ones (Table 2).

Table 2. Theoretical and experimental[a] foci positions and add powers of the Acriva Trinova IOL (20 D)

Focus	Position (D)		Addition (D)	
	Theorical	Experimental	Theorical	Experimental
Near	23.0	22.9	3.0	2.7
Intermediate	21.5	21.5	1.5	1.3
Distance	20.0	20.2		

[a]Values obtained with 3.0 mm pupil

The desired add power P_d imposes the periodicity T of the sinusoidal patterns (r^2 space) through Eq. (4). Then, the sinusoidal profiles shown in Figs. 1 and 2 have the same periodicity (T=0.733 mm^2, intended for P_d=1.5 D) even though they were generated with two different models. On the other hand, the choice of either Model 1 or Model 2 do have significant implications in:

- The mathematical functions that govern the diffraction efficiency of the m=0, and ±1 orders, Bessel functions (Eq. (7)) for Model 1 versus complete elliptic integrals (Eqs. (12) and (13)) for Model 2, which in turns determine the modulation or step height of the diffractive profile necessary to achieve a particular energy split ratio among the orders.
- The topography and radius of the first diffractive zone (compare Figs. 1 and 2 in the vicinity of radius r=0 mm, i.e., the lens centre).

With regard to the diffraction efficiency, we have shown that with both sinusoidal models, it is possible to achieve the condition $\eta_0 = \eta_{\pm 1}$ to have three orders (foci) with the same energy.

Biomedical Optics EXPRESS

Model 1 leads to efficiencies of 30% while Model 2 reaches slightly better ones of 30.8%. It is noteworthy that in comparison to the binary profile, the two sinusoidal ones would ideally allocate more useful energy for the vision process (90% to 92.4% for the sinusoidals versus 86.4% for the binary). Fulfilling the condition of equal diffraction efficiency of the three foci turns out to determine the value of the modulation of the sinusoidal phase functions -β parameter Eq. (3) for Model 1, and $tan^{-1}(\alpha)$ Eq. (9) for Model 2- and so it does with the maximum step height $h_{\max}$ of the diffractive profiles. The findings with both sinusoidal models, along with the experimental results, are summarized in Table 3 and evidence that Model 2 requires 16% shallower diffractive steps than Model 1 (0.84 μm versus 1.00 μm) which is closer to the experimental step height (0.78 ± 0.01 μm) measured in the Acriva Trinova IOL.

Table 3. Maximum Step height h_{max} and radius r_1 of the first diffractive zone

	Experimental[a]	Theoretical		
		Model 1[b]	Model 2[c]	Model 2 with S[d]
$h_{\max}$ (μm)	0.78 ± 0.10	1.00	0.84	0.84
r_1 (mm)	0.70 ± 0.02	0.61	0.74	0.70

[a]Values obtained with confocal and optical microscopy in the Acriva Trinova IOL (20D).
[b]Sinusoidal diffractive profile given by Eq. (8) [18] with β=1.4376 rad, to have $\eta_0 = \eta_{\pm 1}$ (λ=550 nm, n_L=1.462, n_A=1.336, P_d=1.5 D, and T=0.733 mm^2).
[c]Sinusoidal diffractive profile given by Eq. (10) [19] with α=2.65718 to have $\eta_0 = \eta_{\pm 1}$ (λ=550 nm, n_L=1.462, n_A=1.336, P_d=1.5 D, and T=0.733 mm^2).
[d]Sinusoidal diffractive profile with shift parameter given by Eq. (15) [24] with S=+0.307 mm^2 (α=2.65718, λ=550 nm, n_L=1.462, n_A=1.336, P_d=1.5 D, and T=0.733 mm^2)

The topography of the Acriva Trinova IOL, as experimentally measured by confocal microscopy (Figs. 4 and 5(b)) reveals a sinusoidal profile of the outer diffractive zones with a depressed pretty flat central one. The latter is a distinct feature that is not well reproduced either with Model 2 (Fig. 2) nor certainly with Model 1 (Fig. 1). In addition, the radius r_1 of this zone deduced with both models (0.61 mm Model 1, and 0.74 mm Model 2) does not accurately match the experimental value of 0.70 ± 0.02 mm measured in the Acriva Trinova IOL, the latter being in excellent agreement with the data reported by the manufacturer (Table 1).

These two issues are fixed with the generalized form of Model 2 (Eq. (15)) which introduces a shift S of the diffractive profile along the radial direction (r^2 space). As shown in Fig. 3, there are two S values (one positive and one negative) that allow to match the radius r_1 of the first diffractive zone to the experimentally measured and reported by the manufacturer value of 0.70 mm.

However, the theoretical profile shape with the negative S shift strongly departs from the experimental shape measured for the Acriva Trinova IOL by confocal microscopy, the latter being much closer to the theoretical profile predicted by Model 2 with positive S shift. In addition, this parameter also influences the light distribution among the foci [24]. More in concrete, a positive S shift produces that the step of the first diffractive zone has negative slope (see Fig. 3), which allows to allocate more energy to the m=-1 order (i.e., the distance focus) compared to an equal-energy distribution in the tree IOL foci. This fact is consistent with the light distribution in photopic conditions provided by the manufacturer (Table 1) and our experimental results with the 3.0mm pupil (Fig. 8) that show somehow larger EE of the distance focus.

Finally, further theoretical and experimental work is required to determine the chromatic performance of the foci generated by the sinusoidal diffractive design in polychromatic light. For instance, while conventional multifocal IOLs use either 0^{th} or $+1^{st}$ diffraction orders for the distance focus, the sinusoidal one uses diffractive order -1^{st} that induces chromatic aberration of the same sign (positive) that the one due to the refractive base lens. On the other hand, the Acriva Trinova IOL has a high Abbe Number (Table 1), which must mitigate the contribution of the

Biomedical Optics EXPRESS

refractive base lens to the chromatic aberration. All these facts have to be thoroughly analyzed to response the question whether the quality of the foci of the Acriva Trinova IOL (specially the distance one) can be compromised by the chromatic aberration.

5. Conclusions

Two theoretical sinusoidal diffractive profiles (equienergetic and *optimum triplicator*) have been studied. The *optimum triplicator* produce three diffraction orders useful for distance, intermediate and near vision with slightly higher overall efficiency than the equienergetic sinusoidal profile (92.4% vs. 90% respectively). The topographic features of a commercially IOL with a sinusoidal profile, the Acriva Trinova lens, have been measured by confocal microscopy. The trough-focus energy efficiency of the lens has been experimentally assessed and showed a smooth distribution with slightly more energy allocated to the distance focus. The experimental results obtained in the Acrinova Trinova IOL, radii and shape of the diffractive zones, as well as the height of the diffractive steps, match accurately with the ones derived from the *optimum triplicator* upon introducing a positive radial shift in the diffractive profile. Moreover, this generalized profile is expected to favor the distance focus in terms of energy efficiency as experimentally observed.

Funding. Ministerio de Economía y Competitividad (DPI2016-76019-R) and European Union ERDF Funds (DPI2016-76019-R).

Disclosures. The authors have no proprietary or commercial interest in any material or method discussed in this article. M.S. Millán reports grants from Bausch + Lomb, France and OfthalTECH SOLUTIONS, Spain outside the submitted work. F. Vega, M. Valentino and F. Rigato have nothing to disclose.

Data availability. Data underlying the results presented in this paper are not publicly available at this time but may be obtained from the authors upon reasonable request

References

1. D. R. H. Breyer, H. Kaymak, T. Ax, F. T. A. Kretz, G. U. Auffart, and P. R. Hagen, "Multifocal intraocular lenses and extended depth of focus intraocular lenses," Asia-Pac. J. Ophthalmol. **6**(4), 339–349 (2017).
2. G. Monaco, M. Gari, F. DiCenso, A. Poscia, G. Ruggi, and A. Scialdone, "Visual performance after bilateral implantation of 2 new presbyopia-correcting intraocular lenses: trifocal versus extended range of vision," J. Cataract Refractive Surg. **43**(6), 737–747 (2017).
3. B. Cochener, G. Boutillier, and M. Lamard, "A comparative evaluation of a new generation of diffractive trifocal and extended depth of focus intraocular lenses," J. Refract. Surg. **34**(8), 507–514 (2018).
4. R. Mencucci, E. Favuzza, O. Caporossi, A. Savastano, and S. Rizzo, "Comparative analysis of visual outcomes, reading skills, contrast sensitivity, and patient satisfaction with two models of trifocal diffractive intraocular lenses and an extended range of vision intraocular lens," Graefe's Arch. Clin. Exp. Ophthalmol. **256**(10), 1913–1922 (2018).
5. S. Escandón-Garcia, F. J. Ribeiro, C. McAlinden, A. Queirós, and J. M. Gonzalez-Méijome, "Through focus vision performance and light disturbances of 3 new intraocular lenses for presbyopia correction," J. Opthalmol., 6165493 (2018).
6. F. Castignoles, M. Flury, and T. Lepine, "Comparison of the efficiency, MTF and chromatic properties of four diffractive bifocal intraocular lens designs," Opt. Express **18**(5), 5245–5256 (2010).
7. F. Vega, F. Alba-Bueno, and M. S. Millán, "Energy distribution between distance and near images in apodized diffractive multifocal intraocular lenses," Invest. Ophthalmol. Visual Sci. **52**(8), 5695–5701 (2011).
8. M. Sokolowsky, J. Pniewski, R. Brygola, and M. Kowalczyk-Hernández, "Hybrid heptafocal intraocular lens," Optica Applicata XLV **3**, 285–298 (2015).
9. M. S. Millán, F. Vega, and I. Ríos-López, "Polychromatic image performance of diffractive bifocal intraocular lenses: Longitudinal chromatic aberration and energy efficiency," Invest. Ophthalmol. Visual Sci. **57**(4), 2021–2028 (2016).
10. Y. Lee, G. Łabuz, H. Son, T. M. Yildirim, R. Khoramnia, and G. U. Auffarth, "Assessment of the image quality of extended depth-of-focus- intraocular lens models in polychromatic light," J. Cataract Refractive Surg. **46**(1), 108–115 (2020).
11. D. Gatinel, C. Pagnoulle, Y. Houbrechts, and L. Gobin, "Design and qualification of a diffractive trifocal optical profile for intraocular lens," J. Cataract Refractive Surg. **37**(11), 2060–2067 (2011).
12. J. Loicq, N. Willet, and D. Gatinel, "Topography and longitudinal chromatic aberration of refractive-diffractive multifocal intraocular lenses," J. Cataract Refractive Surg. **45**(11), 1650–1659 (2019).
13. M. S. Millán and F. Vega, "Extended depth of focus intraocular lens: chromatic performance," Biomed. Opt. Express **8**(9), 4294–4309 (2017).
14. F. Vega, M. S. Millán, N. Garzón, M. A. Gil, and F. Rigato, "Features of the optical surface of an extended depth of focus intraocular lens," *presented at the 37th Congress of the ESCRS*, Paris, France, 14–18 Sept. 2019.

Biomedical Optics EXPRESS

15. V. Osipov, L. L. Doskolovich, E. A. Bezus, T. Drew, K. Zhou, K. Sawalha, G. Swadener, and J. S. S. Wolffsohn, "Application of nanoimprinting technique for fabrication of trifocal diffractive lens with sine-like radial profile," J. Biom. Opt. **20**(2), 025008 (2015).
16. A. L. Cohen, "Practical design of a bifocal hologram contact lens or intraocular lens," Appl. Opt. **31**(19), 3750–3754 (1992).
17. V. Moreno, J. F. Román, and J. R. Salgueiro, "High efficiency diffractive lenses: deduction of kinoform profile," Am. J. Phys. **65**(6), 556–562 (1997).
18. P. J. Valle, J. E. Oti, V. F. Canales, and M. P. Cagigal, "Visual axial PSF of diffractive trifocal lenses," Opt. Express **13**(7), 2782–2792 (2005).
19. F. Gori, M. Santarsiero, S. Vicalvi, R. Borghi, G. Cincotti, E. Di Fabrizio, and M. Gentili, "Analytical derivation of the optimum triplicator," Opt. Commun. **157**(1-6), 13–16 (1998).
20. VSY Biotechnology, The Netherlands, "Acriva Trinova product brochure," https://www.vsybiotechnology.com/acriva-trinova/.
21. A. Amigó-Francés, A. Castillo-Gómez, D. Carmona-González, P. Martínez-Sorribes, and A. Amigó, "Comparative study of visual results obtained with two trifocal lens models in cataract surgery," Arch. Clin. Exp. Ophthalmol. **2**(2), 054–060 (2020).
22. A. L. Cohen, "Diffractive bifocal lens design," Optom. Vis. Sci. **70**(6), 461–468 (1993).
23. M. Abramowitz and I. Stegun eds., *Handbook of Mathematical Functions* (Dover, 1972).
24. S.T.S Holmström, I Çim, and H. Urey, "An ophthalmic multifocal diffractive lens," European Patent Specification 3435143B1 (1 April 2020).
25. International Organization for Standardization, ISO 11979–2:2014 "Ophthalmic Implants - Intraocular Lenses - Part 2: Optical Properties and Test Methods," Geneva; ISO. (2014).
26. A. Guirao, M. Redondo, and P. Artal, "Optical aberrations of the human cornea as a function of age," J. Opt. Soc. Am. A **17**(10), 1697–1702 (2000).
27. L. Wang, E. Dai, D. D. Koch, and A. Nathoo, "Optical aberrations of the human anterior cornea," J. Cataract Refractive Surg. **29**(8), 1514–1521 (2003).
28. L. N. Thibos, X. Hong, A. Bradley, and R. A. Applegate, "Accuracy and precision of objective refraction from wavefront aberrations," J. Vis. **4**(4), 9–351 (2004).
29. S. Ravikumar, A. Bradley, and L. N. Thibos, "Chromatic aberration and polychromatic image quality with diffractive multifocal intraocular lenses," J. Cataract Refractive Surg. **40**(7), 1192–1204 (2014).
30. J. Armengol, N. Garzon, F. Vega, I. Altemir, and M. S. Millán, "Equivalence of two optical quality metrics to predict the visual acuity of multifocal pseudophakic patients," Biomed. Opt. Express **11**(5), 2818–2829 (2020).
31. G. A. Lenkova, "Diffractive-Refractive intraocular lenses with binary structures," Optoelectro., Instrum. Data Process. **54**(5), 469–476 (2018).
32. G. A. Lenkova, "Features of optical surfaces of multifocal diffractive-refractive eye lenses," Optoelectro., Instrum. Data Process. **53**(5), 431–441 (2017).
33. A. Voskresenskaya, N. Pozdeyeva, N. Pahtaev, Y. Batkov, V. Treushnicov, and V. Cherednik, "Initial results of trifocal diffractive IOL implantation," Graefe's Arch. Clin. Exp. Ophthalmol. **248**(9), 1299–1306 (2010).